





Open Archive Toulouse Archive Ouverte (OATAO)

OATAO is an open access repository that collects the work of Toulouse researchers and makes it freely available over the web where possible

This is an author's version published in: <http://oatao.univ-toulouse.fr/25133>

Official URL: <https://doi.org/10.1021/acs.langmuir.6b03584>

To cite this version:

Nyame Mendendy Boussambe, Gildas  and Valentin, Romain  and Fabre, Jean-François  and Navailles, Laurence and Nallet, Frédéric and Gaillard, Cédric and Mouloungui, Zéphirin  *Self-Assembling Behavior of Glycerol Monoundecenoate in Water*. (2017) *Langmuir*, 33 (13). 3223-3233. ISSN 0743-7463

Any correspondence concerning this service should be sent to the repository administrator: tech-oatao@listes-diff.inp-toulouse.fr

Self-Assembling Behavior of Glycerol Monoundecenoate in Water

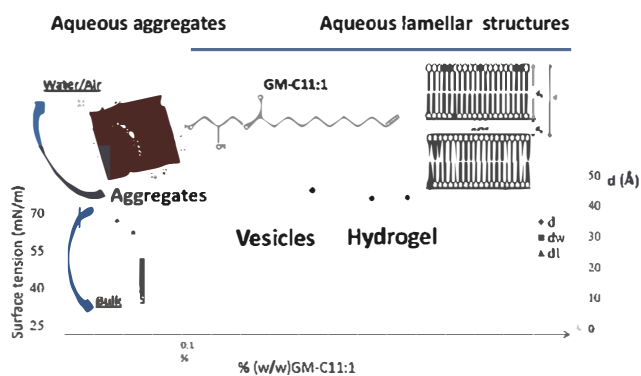
Gildas Nyame Mendendy Boussambe,[†] Romain Valentin,^{*,†,‡} Jean-François Fabre,[†] Laurence Navailles,[‡] Frédéric Nallet,[‡] Cédric Gaillard,[§] and Zéphirin Mouloungui[†]

[†]Laboratoire de Chimie Agro Industrielle (LCA), Université de Toulouse, INRA, INPT, 31030 Toulouse, France

[‡]Centre de Recherche Paul Pascal, CNRS, Université de Bordeaux, 33600 Pessac, France

[§]UR 1268 Biopolymères Interactions et Assemblages, INRA, rue de la Géraudière, 44316 Nantes, France

ABSTRACT: The self assembling properties of glycerol esters in water are well known. Still, few data on glycerol monoesters of undecylenic acid are available. The aim of this study was to highlight the behavior of glycerol monoundecenoate (GM C11:1) in different diluted and concentrated states. Its self assembling properties in water and upon solid inorganic surfaces were investigated in the diluted state using surface tension experiments, atomic force microscopy, and cryogenic transmission electron microscopy studies. In the concentrated state, the gelling properties in the presence of water were investigated using polarized light microscopy, differential scanning calorimetry (DSC), and small angle X ray scattering (SAXS) experiments. GM C11:1 at 100 mg/L self assembles at the liquid/air interfaces as aggregates of approximately 20 nm in diameter, organized into concentric forms. These aggregates are spherical globules composed of several molecules of GM C11:1. At higher concentrations (1000 and 10⁴ mg/L), GM C11:1 is able to uniformly coat liquid/air and liquid/solid interfaces. In bulk, GM C11:1 forms spontaneously aggregates and vesicles. In a more concentrated state, GM C11:1 assembles into lamellar L_β and L_α forms in water. By cross referencing SAXS and DSC findings, we were able to distinguish between interlamellar water molecules strongly bound to GM C11:1 and other molecules remaining unbound and considered to be “mobile” water. The percentage of water strongly bound was proportional to the percentage of GM C11:1 in the system. In this case, GM C11:1 appears to be an effective molecule for surface treatments for which water retention is important.



INTRODUCTION

The replacement of building block molecules of fossil origin is currently a major issue. Biomass¹ and plant oils in particular² are possible alternative sources of these molecules. Castor oil is rich in ricinoleic acid, which accounts for 90% of the fatty acids present. Undecylenic acid can be obtained using the pyrolysis of castor oil or of the methyl ester of castor.³ This biosourced chemical building block molecule is of particular interest because it carries two reactive functional groups. It has a reactive carboxylic acid group, from which glycerol mono undecenoate (GM C11:1) can be synthesized, and an alkene group, the chemistry of which is currently being studied.³ The molecules generated from undecylenic acid are of interest in terms of their reaction potential, as discussed by Bigot et al.,⁴ and the potential physicochemical properties conferred by the polar and lipophilic parts of the molecules in each generation.

In this study, we focused on GM C11:1, the first generation of molecules obtained from the reaction of undecylenic acid with glycerol. This amphiphilic molecule has a polar head composed of glycerol and a lipophilic tail consisting of undecylenic acid. Monoglycerides account for 75%, by volume, of the emulsifiers produced worldwide,⁵ and these molecules

are widely used in diverse applications in cosmetics, pharmaceutical, and food products. Their ability to self assemble is a much sought after feature, and their behavior in water has been extensively studied over many years. These molecules self assemble in water,⁶ forming aggregates,⁷ vesicles,^{8,9} and organized cubic, lamellar, and hexagonal phases.⁵ Each type of monoglyceride displays its own specific behavioral pattern,¹⁰ although generalizations have been made for saturated and monounsaturated monoglycerides.¹¹ In general, the melting points of monoglycerides and aqueous gels (Krafft temperature) increase with chain length.^{12,13} Monoglycerides are used as stabilizers for emulsions,¹⁴ particularly in cosmetics, as structuring agents in the agrofood industry¹⁵ and as phytosanitary products.¹⁶

GM C11:1 differs from the monoglycerides often described in published studies and commonly used in industry in that it consists of an alkyl chain with an odd number of carbons and terminal unsaturation (Figure 1), with the terminal double

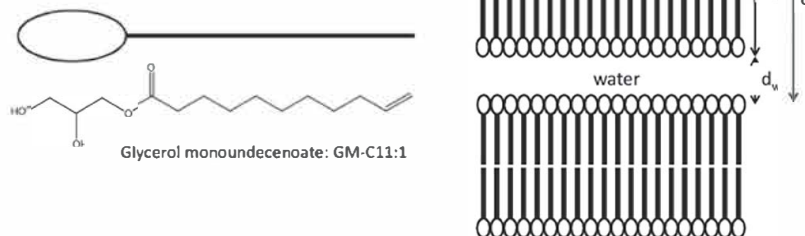


Figure 1. Schematic representation of a lamellar phase.

bond conferring a certain degree of mobility to the molecule. Few studies have investigated the ability of this molecule to self assemble. Many studies have addressed the issue of the physicochemical behavior of monoglycerides with even number of carbons, and irregularities have been identified for a series of monoglycerides with even and odd numbers of carbons in their saturated alkyl chains (C14–C18).¹⁷ For GM C11:1, it has been shown that surfaces covered with mixtures of glycerol monolaurate and GM C11:1 become superhydrophilic through the formation of a hydrogel.¹⁸

In this study, we investigated the physicochemical behavior of GM C11:1 in more detail. Using tensiometry, cryogenic transmission electron microscopy (cryo TEM), and atomic force microscopy (AFM), we investigated the adsorption of GM C11:1 in dilute solutions onto liquid/air and liquid/solid interfaces. Differential scanning calorimetry (DSC) and small angle X ray scattering (SAXS) studies were also carried out to determine whether high concentration preparations of GM C11:1 displayed the same organization in water as some of the monoglycerides described in previous studies or whether they displayed a specific, different type of behavior because of the odd number of carbons in the alkyl chain and the presence of the terminal double bond.

EXPERIMENTAL SECTION

Materials. Glycerol (98%) was obtained from Sigma Aldrich, undecylenic acid (99%) was purchased from Acros Organic, and dodecylbenzene sulfonic acid ($\geq 95\%$) was obtained from Sigma Aldrich. High performance liquid chromatography quality solvents (cyclohexane, ethyl acetate, chloroform, and methanol) were obtained from Aldrich.

GM C11:1 was synthesized by the esterification of undecylenic acid and glycerol. It was then purified on a silica column, according to the procedure developed by Boussambe et al.¹⁹ The preparation was shown to be 99% pure, using gas chromatography and ¹H NMR. The GM C11:1 preparation was a mixture of the isomers 1 glycerol monoundecenoate (92.3% molar) and 2 glycerol monoundecenoate (7.7% molar), as shown by ¹H NMR. The NMR spectrum obtained is presented in the [Supporting Information](#).

Silica SIPERNAT 2200 was purchased from Degussa and used as received. The specific surface area (N_2), in accordance with the ISO 9277 standard, was 190 m²/g.

Surface Tension Experiments. Surface tension (γ) measurements at the air/water interface were taken on a GBX 3S (France) surface tensiometer, using the Wilhelmy plate method. The instrument was calibrated and checked by measuring the surface tension of Milli Q water before each experiment. We added aliquots of known volumes to 25 mL of water and measured γ (mN/m) in each case. The solution was gently stirred and allowed to equilibrate for 10 min before any measurements were taken, and each measurement was performed at least three times. The temperature was maintained at 25 °C.

Polarized Light Microscopy. Observations were made using a Nikon Edipse E600 light microscope (Nikon Corporation, Japan) equipped with polarized filters and a Mettler Toledo FP82HT hot stage controlled by an FP90 central unit. The images were acquired with a high resolution, low noise Nikon DXM 1200 color CCD camera and were analyzed using LUCIA G version 4.8 software.

Cryogenic Transmission Electron Microscopy. Specimens for cryo TEM observation were prepared using a cryoplunge cryo fixation device (Gatan, USA) in which a drop of the aqueous suspension was deposited onto glow discharged holey type carbon coated grids (Ted Pella Inc., USA). The TEM grid was then prepared by blotting the drop containing the specimen to a thin liquid layer that remained across the holes in the support carbon film. The liquid film was vitrified by rapidly plunging the grid into liquid ethane cooled by liquid nitrogen. The vitrified specimens were mounted on a Gatan 910 specimen holder (Gatan, USA) that was inserted in the microscope using a CT 3500 cryotransfer system (Gatan, USA) and cooled with liquid nitrogen. TEM images were then obtained from specimens preserved in vitreous ice and suspended across a hole in the supporting carbon substrate.

All samples were observed under a JEM 1230 cryomicroscope (JEOL, Japan) operated at 80 kV and equipped with a LaB₆ filament. For cryo TEM experiments, the microscope was operated under low dose conditions ($<10 \text{ e}^-/\text{Å}^2$) while maintaining the sample at -178 °C . The micrographs were recorded on a Gatan 1.35k \times 1.04k \times 12 bit ESS00W CCD camera.

Adsorption of GM-C11:1 at the Liquid/Solid Interface. Adsorption isotherms at 25 °C were established by measuring the concentration of the solution of GM C11:1 in water before and after adsorption on silica. Determinations were based on UV absorption, measured using a Shimadzu UV 1800. We added approximately 0.5 g of silica to 10 g of a GM C11:1 solution of known initial concentration. Once equilibrium was reached, we separated the solid from the solution by passage through cellulose acetate filters with 22 μm pores.

DSC Experiments. The analyses were performed using a Mettler Toledo System DSC1 STAR^c machine (Perkin Elmer, USA) equipped with an internal cooling system. The device was purged with nitrogen, at a flow rate of 20 mL/min. Indium ($T_m = 156.68 \text{ °C}$ and $\Delta H_f = 28.45 \text{ J/g}$) and distilled water ($T_m = 0 \text{ °C}$ and $\Delta H_f = 333.79 \text{ J/g}$) were used for calibration. The data were analyzed using STAR^c evaluation software (Mettler Toledo). Samples of known mass (in milligrams) were weighed in an aluminum crucible, to the nearest 0.1 mg. The crucible was then hermetically sealed with an aluminum cover. A hermetically sealed empty aluminum crucible was used as the reference. The thermal history of the samples was erased by heating each sample to 50 °C for 5 min before analyzing thermal behavior. The samples were subjected to two cycles of cooling and heating, from 50 to -80 °C at a cooling and heating rate of 5 °C/min.

Atomic Force Microscopy Experiments. Langmuir–Blodgett (LB) films for AFM observation were performed using a MicroTrough LB trough (Kibron Inc., Helsinki, Finland). The GM C11:1 aqueous solution at a given concentration was spread at 20 °C on the surface of water with a microsyringe and the solvent was let to evaporate. The

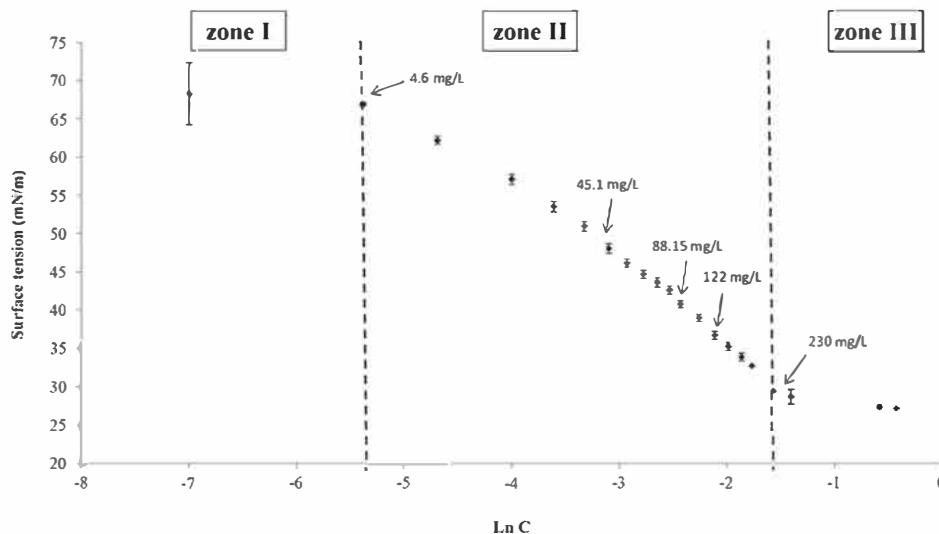


Figure 2. Surface tension as a function of the natural logarithm of concentration (g/L) at 25 °C.

surface was compressed at a speed of $100 \text{ cm}^2 \text{ min}^{-1}$. At a surface pressure of 20 mN/m , the film at the air/water interface was transferred onto a mica sheet at a speed of 0.1 mm/s .

The Langmuir films were air dried and imaged using AFM over an area of 500 nm^2 to $20 \text{ }\mu\text{m}^2$ at 0.2 to 0.5 Hz operated in the PeakForce Tapping mode using a BioScope Catalyst AFM (Bruker AXS, Santa Barbara, CA) and a set point of around $1\text{--}2 \text{ nN}$. ScanAsyst Air AFM tips (Bruker AFM Probes, Camarillo, CA) were used for each experiment with a nominal spring constant, resonant frequency, and radius of 0.4 N/m , 70 kHz , and 2 nm , respectively. AFM data were analyzed using the NanoScope Analysis 1.5 software (Bruker AXS, Santa Barbara, CA).

SAXS Experiments. SAXS experiments were performed using an HI. NanoStar device (from Bruker) with point collimation and a radiation wavelength of $\lambda = 1.5418 \text{ \AA}$. Experiments were performed under vacuum, at controlled temperatures, and a 2D gas detector (HISTAR, also from Bruker; 1024×1024 pixels, with a pixel size of $100 \text{ }\mu\text{m}$) was used to record the spectra. The sample to detector distance was 25.5 cm , calibrated using a silver behenate standard. The processed data were normalized by acquisition time and corrected by subtracting the spectrum of water as background, taking into account transmissions. The prepared samples were transferred to quartz capillary tubes (1.5 mm in diameter), which were then sealed and stored at $-80 \text{ }^\circ\text{C}$. SAXS acquisitions were performed at 70 and $5 \text{ }^\circ\text{C}$.

The structural parameters were calculated from the repeat period (d), assuming lamellar symmetry and planar bilayers in converting measured Bragg peak position (q_0) to d , namely, $d = 2\pi/q_0$. The penetration of water into the lipid bilayer and the dissolution of lipid in the water layer were assumed to be negligible. The repeat period d was separated into a lipid bilayer thickness d_1 and a water layer thickness d_w , calculated in the conventional manner^{20,21}

$$d_1 = \frac{(1-c) \times v_1}{(1-c) \times v_1 + c \times v_w} \times d$$

$$d = d - d_w$$

where c is the fraction of water by weight, and v_1 and v_w are the partial specific volumes of GM C11:1 and water, respectively (Figure 1). We used $v_w = 1 \text{ cm}^3/\text{g}$. The partial specific volume of GM C11:1 was assumed to be $1.04 \text{ cm}^3/\text{g}$ ($\rho = 0.96 \text{ g/cm}^3$).

The area per lipid molecule at the water interface can also be calculated

$$A = \frac{2 \times V_M}{d}$$

V_M is the molecular volume of GM C11:1: $V_M = Mv_1/N$, where M is the molecular weight of GM C11:1 and N is Avogadro's number.

RESULTS AND DISCUSSION

Behavior of Dilute GM-C11:1. The ability of GM C11:1 to reach interfaces was first evaluated by measuring its capacity to decrease the air/water interfacial tension. Surface tension at the water/air interface was plotted against the natural logarithm of GM C11:1 concentration (Figure 2).

Zone I corresponds to very dilute solutions of GM C11:1. At these very low concentrations, the molecules of GM C11:1 are too far apart to have any effect on surface tension. In zone II, surface tension decreases rapidly because of the accumulation of GM C11:1 molecules at the surface. This decrease is not strictly linear, and three changes in slope are evident, at 41.1 , 88.15 , and 122 mg/L . Surface tension stabilizes in zone III at less than 30 mN/m because the surface becomes saturated with GM C11:1. In this zone, the GM C11:1 solutions are cloudy. GM C11:1 may have limited solubility or may form dispersed objects in water that are large enough to scatter light by Tyndall effect.

The curve in Figure 2 resembles those obtained by Queste et al. for glycerol ethers²² and by Lunkenheimer et al. for ethers of n alkanols,²³ for which the nonlinear decrease in surface tension in zone II is characterized by the solvo surfactant behavior, with molecules forming interacting aggregates as their concentrations increase. Indeed, if GM C11:1 adsorbed onto the air/water interface molecule by molecule, the molecular area could be calculated using the Gibbs equation

$$\Gamma = \left(\frac{1}{mRT} \right) \left(\frac{d\gamma}{d \ln C} \right)_{T,P}$$

where Γ is the surface excess, R is the ideal gas constant, T is the temperature in kelvins, $d\gamma/d \ln C$ is the slope of the curve in zone II (Figure 2), at a constant temperature T and a constant pressure P , and m is the number of species present.

According to this equation, the molecular area would be close to 48.9 \AA^2 . This value is very different from the molecular area of 11 \AA^2 calculated using modeling (Figure 3), taking into account the influence of water on the geometry optimization of the GM C11:1 molecule. It is also much higher than the values obtained for glycerol monolaurate from compression isotherms

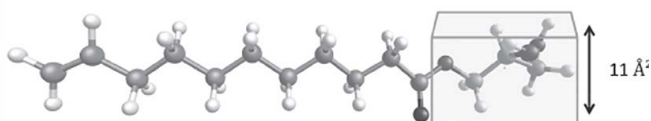


Figure 3. Molecular modeling of GM C11:1 by mechanical modeling (MM3) and then semiempirical modeling (PM6) with implicit water modeling (COSMO).

at Langmuir equilibrium.²⁴ At a surface tension of 32 mN/m, the molecular area of glycerol monolaurate is approximately 10 Å². This difference may mean that in Gibbs equation, the value of Γ is overestimated for $m = 1$, as is the case for insoluble nonionic surfactants, in a monomolecular form, in water. If GM C11:1 self assembles in solution as aggregates capable of adsorbing onto the surface, then the value of m will be greater than 1. The mean value of m would need to be approximately 3.3 to obtain a molecular area of 11 Å², consistent with molecular models.

This theoretical approach was tested using cryo TEM imaging on GM C11:1 solutions in zone III of Figure 2. A thin aqueous film from the sample dispersion was vitrified in liquid ethane to obtain a fixed image of the assembly of molecules in a solution of the given concentration. Zone III was reached at a concentration of 1000 mg/L. In Figure 4a, we can

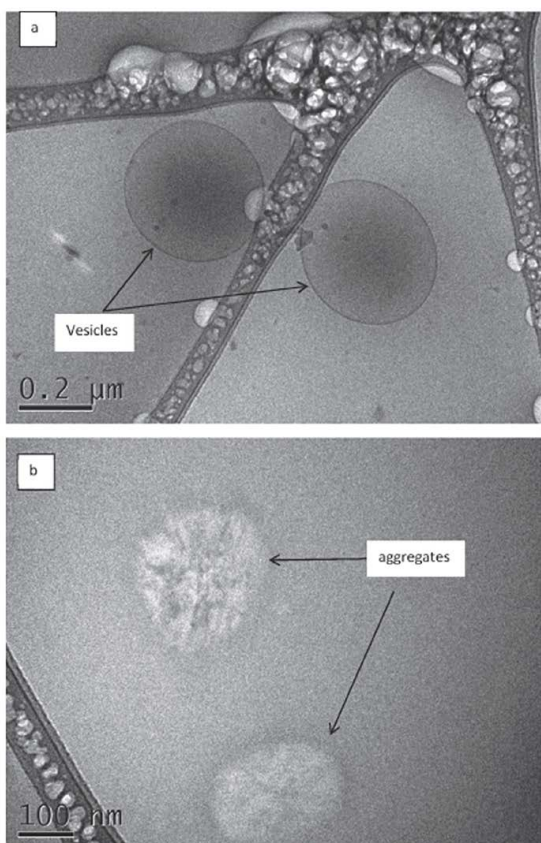


Figure 4. Cryo TEM of a 1000 mg/mL GM C11:1 solution.

see an object consisting of a dark circle with a very dark circumference. This dark circumference results from the diffusion of electrons in the part of the beam hitting the largest expanse of the wall of the object, an observation often characteristic of liposomes.^{25,26} The dark zone in the center of the circle is typical of a spherical object, such as a vesicle, with a

diameter of approximately 500 nm. In Figure 4b, flat aggregates in the form of oval discs of approximately 100–300 nm in diameter are also present. Cryo TEM analysis, as in the work of Klaus et al.,²⁷ can be used to highlight micelles of more than 7 nm diameter. In our sample, no evidence was found of the presence of big micellar structure resembling that potentially expected if the point between zones II and III corresponded to the critical micellar concentration (CMC). In the experimental conditions, no micelle was observed. This implies that the micelles are either absent or not visible. These proposals are in line with the aggregation of GM C11:1 in the aqueous phase to generate objects adsorbed at the liquid/air interface. This behavior could be attributed to a lack of hydrophilicity of the polar head. In the case of GM C11:1, the intersection of zones II and III corresponds to the threshold concentration above which the surface is saturated with GM C11:1. Beyond this critical aggregation concentration (CAC), GM C11:1 assembles into aggregates and vesicles with a large diameter. The presence of these objects accounts for the cloudiness of the solutions observed in zone III.

These objects are generated spontaneously, at room temperature, without the need for other constituents. The images in Figure 4a show that the vesicles formed are of similar dimensions and appearance to the lamellar vesicles prepared from phospholipid bilayers and stabilized with ethoxylated copolymers.²⁸ These systems are of considerable interest for many applications, including drug delivery, for which vesicular systems prepared from nonionic molecules present several major advantages, particularly in terms of stability. For most of the nonionic surfactants tested, the generation of such vesicles, also known as niosomes, has been shown to require cholesterol. Bilayer fluidity is increased by the presence of cholesterol, favoring the formation of vesicular structures.²⁹ The self assembly of GM C11:1, therefore, appears to require no external assistance, and there seems to be sufficient fluidity for the formation of vesicles. This fluidity may be due to the presence of the terminal double bond, which increases the flexibility of the alkyl chain.

Surface Morphology on AFM. The LB technique is widely used to produce and study using AFM the structure of molecular organization at the air/water interface. Transferring lipid structures at constant surface pressure and constant speed onto mica surfaces was undertaken with a careful control of surface pressure and lifting speed to avoid artifacts such as defect formation or feature alignment of the deposited structures. However, we assume that lipid molecules interact fast and strongly with mica surface so that the structures are fixed stable in air, not in water, and should therefore be examined in air using AFM. This technique is proven to observe the state of the interfaces without notable modification of the interfacial organization.³⁰ By this way, we surveyed the fine organization of GM C11:1 at the air/water interface as a function of the initial dispersion concentration. It has been shown that glycerol monooleate, glycerol monopalmitate, and glycerol monolaurate, in the form of Langmuir films, confer a certain rigidity on the liquid/air interface, via different mechanisms, depending on the nature of the alkyl chain.³¹ A film of glycerol monopalmitate, for example, forms a dense, brittle crystalline structure before collapse, whereas glycerol monooleate forms a more expansive, nonbrittle structure.³² This difference is due principally to differences in repulsive hydration forces between these two types of monoglycerides.³³

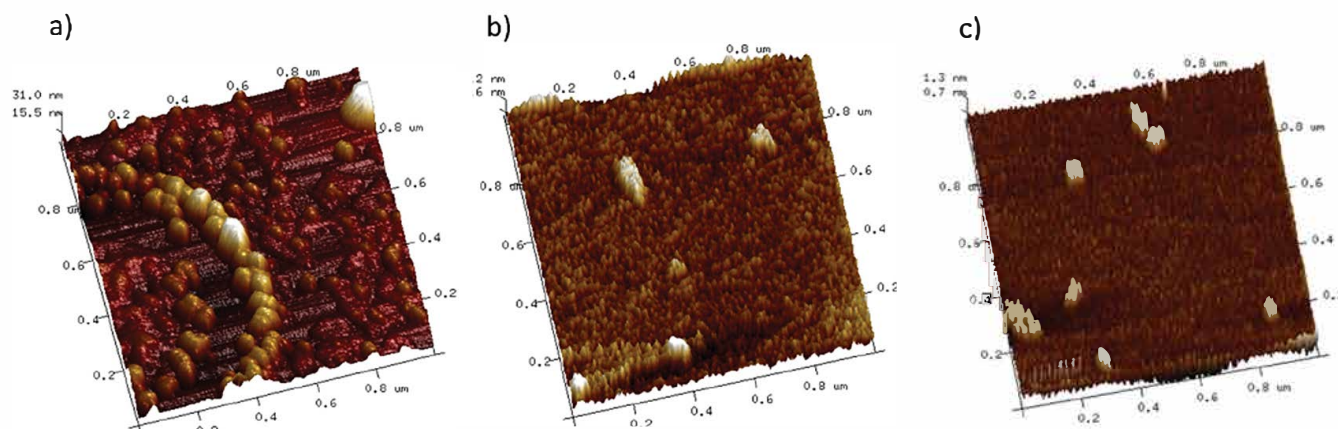


Figure 5. Height AFM images of a solution of GM C11:1 at a concentration of (a) 100, (b) 1000, and (c) 10^4 mg/L.

The liquid/air interfaces of GM C11:1 solutions in zone II, analyzed at a concentration of 0.1 mg/L by AFM (Figure 5), presented aggregates of approximately 20 nm in diameter, organized into concentric forms. These aggregates were spherical globules composed of several molecules of GM C11:1, organized, like polymers, into monolayers.³⁴ There were spaces between globules corresponding to the naked aqueous subphase, as the concentration was not sufficiently high for surface saturation. At higher concentrations (1000 and 10^4 mg/L), in zone III, the surface was evenly coated and presented no defects other than masses of globules that could potentially give rise to an additional layer (Figure 5b,c).

Adsorption at the Liquid/Solid Interface. Many studies have investigated the mechanisms by which amphiphilic molecules adsorb at liquid/solid interfaces. This adsorption plays a key role in many technological and industrial applications, as detergents, in the flotation of minerals, the inhibition of corrosion, and the dispersion of solids, for example.³⁵ The state of the solid surface must be checked in studies of the adsorption of molecules. Hydrophilic surfaces display affinity for water. The chemistry of these surfaces allows them to form hydrogen bonds with water. In general, mineral oxides and silica surfaces are used to study the adsorption of surfactants to hydrophilic surfaces.^{36–41} Thus, to demonstrate the capacity of GM C11:1 to adsorb onto hydrophilic surfaces, we generated an adsorption isotherm for neutral silica particles with interparticle areas of $190 \text{ m}^2 \cdot \text{g}^{-1}$.

The number of molecules of GM C11:1 adsorbed to the silica surface was dependent on the concentration at equilibrium (Figure 6). The adsorption curve obtained was of a shape similar to that obtained for nonionic ethoxylated surfactants. Zone I corresponds to a state in which the amphiphilic molecules are separated by very large distances, and adsorbate–adsorbate interactions are, therefore, negligible. Adsorption in this zone may be due to interactions between the glycerol head of GM C11:1 and the silanols of silica. Zone II corresponds to the saturation of the silica surface with GM C11:1. Adsorbate–adsorbate and adsorbate–adsorbant interactions increase in intensity in this zone. Zone III corresponds to an increase in GM C11:1 adsorption on the silica surface until a plateau is reached. Higher concentrations of GM C11:1 in solution are associated with a greater likelihood of the molecules becoming organized so as to saturate the surface. In zones II and III, the concentration of GM C11:1 exceeds the CAC. It has been defined in the previous section on the GM C11:1 surface activity at the air–/ water interface, that, above

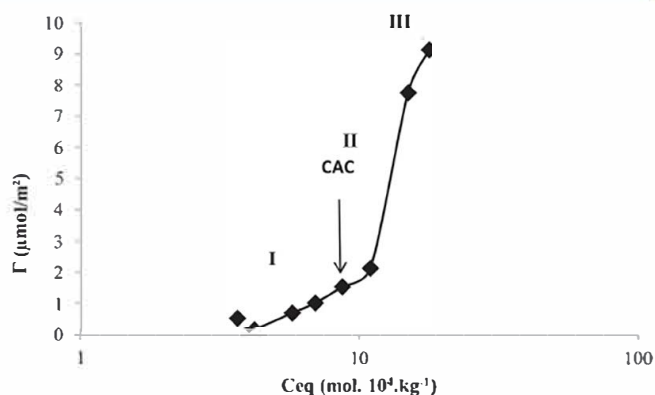


Figure 6. Experimental adsorption isotherm for GM C11:1 at 25 °C on silica.

CAC, GM C11:1 assembles into vesicles and aggregates in solution, and that it covers the liquid/air interface evenly. The position of the CAC on the adsorption isotherm indicates that for adsorption at the liquid/solid interface, the concentration of GM C11:1 must exceed the CAC. The excess molecules not adsorbed at the liquid/air interface are thus adsorbed at the liquid/solid interface.

Using the value for the excess maximum surface attained in Figure 6 ($9.2 \mu\text{mol}/\text{m}^2$), we can calculate the area occupied by a molecule at the liquid/silica interface. The area obtained, 18 \AA^2 , is in the same range of value to that obtained using molecular modeling for a molecule of GM C11:1 in water (Figure 3), and all the more so that the value of excess maximum surface is probably undervalued because the plateau was not reached. GM C11:1, thus, seems to adsorb onto the surface of the silica in the form of a monolayer of individual molecules, consistent with the findings of Partyka et al. concerning the adsorption of nonionic surfactants to silica.⁴¹ The amount of GM C11:1 adsorbed per unit surface area was higher for GM C11:1, at $9 \mu\text{mol}/\text{m}^2$, than for the ethoxylated nonionic surfactants described in previous studies,^{42,43} such as $\text{C}_{12}(\text{EO})_6$ for which an adsorption of $4.5 \mu\text{mol}/\text{m}^2$ was reported. This difference can be accounted for by the lower molecular mass of GM C11:1 when compared with that of ethoxylated surfactants. Final assembly at the surface is very similar for ethoxylated surfactants and GM C11:1, but the mechanisms of adsorption are different. At concentrations above the CMC, ethoxylated surfactants assemble into spherical micelles in solution before their adsorption. Below this

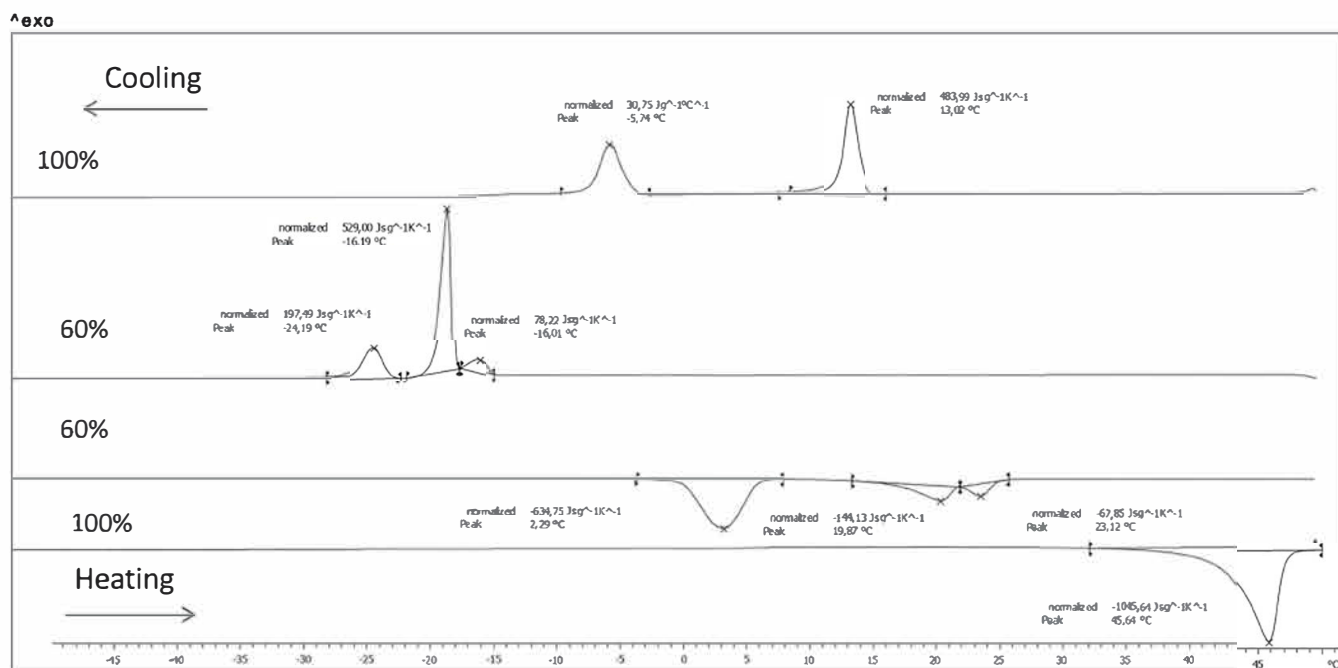


Figure 7. Thermograms for pure GM C11:1 and 60% GM C11:1 in water. Heating and cooling rates of $5^{\circ}\cdot\text{min}^{-1}$ were used.

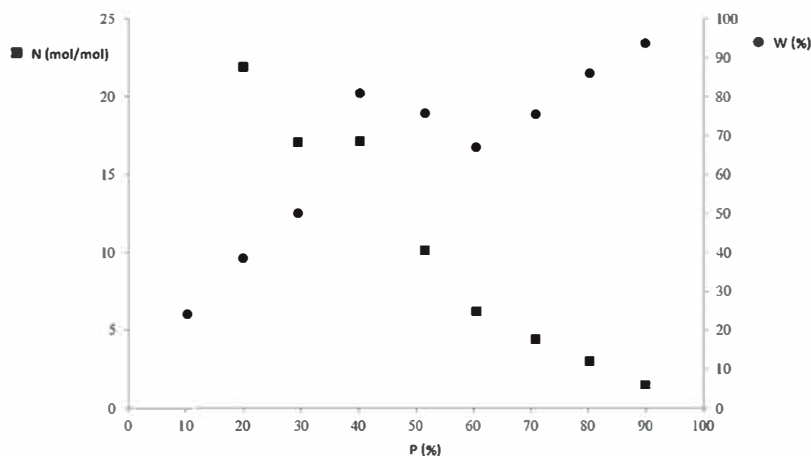


Figure 8. Percentage of strongly bound water molecules (W) and the number of water molecules strongly bound (N), as a function of the percentage of GM C11:1 in water (P).

threshold, they are present in the monomolecular state in solution and adsorb onto the surface molecule by molecule. The molecules of GM C11:1 form aggregates in solution at concentrations below the CAC and form aggregates and vesicles above this concentration. In this state, GM C11:1 adsorbs onto the surface and reorganizes into a monolayer. On the corresponding adsorption isotherms, the positions of the CMCs and CACs are not comparable because these concentrations define different phenomena: saturation of the interface and monomolecular diffusion at the interface for ethoxylated surfactants and saturation of the interface due to the adsorption of molecular aggregates for GM C11:1.

Study of Binary Concentrated Amphiphile/Water Systems. Studies of the polymorphism of pure monoglycerides and of mixtures of monoglycerides have shown that these molecules display very interesting patterns of thermal behavior. They have three crystalline states: α , β' , and β . The β form is the most stable of these crystalline or polymorphic forms, the α and β' forms displaying markedly lower stability.^{44–46}

Monoglycerides form gels in water, under certain conditions (in terms of temperature and heating/cooling rates).^{47–49} They may assemble into different phases—lamellar, hexagonal, cubic—depending on their nature and concentration.¹² This self assembly favors the formation of a structure with water and facilitates two types of interaction between the molecules of the polar solvent and the polar head of the amphiphile. Ambrosi et al.⁵⁰ and Shibukawa et al.⁵¹ showed that the hydration of nonionic surfactants of the alkanoyl 6 *O* ascorbic acid ester type and polymers led to the formation of coagels and gels. The coagel phase may adopt a lamellar L_{β} structure consisting of a stack of layers separated by thin layers of water. This water is, thus, sandwiched between two layers of surfactant, resulting in systems containing a mixture of tightly bound and free water molecules.^{47,51,52} We carried out SAXS and DSC experiments to determine the organization of GM C11:1 in concentrated aqueous solutions.

Study of GM-C11:1/Water Systems by DSC. The thermal history of the samples was cleared by heating to 50

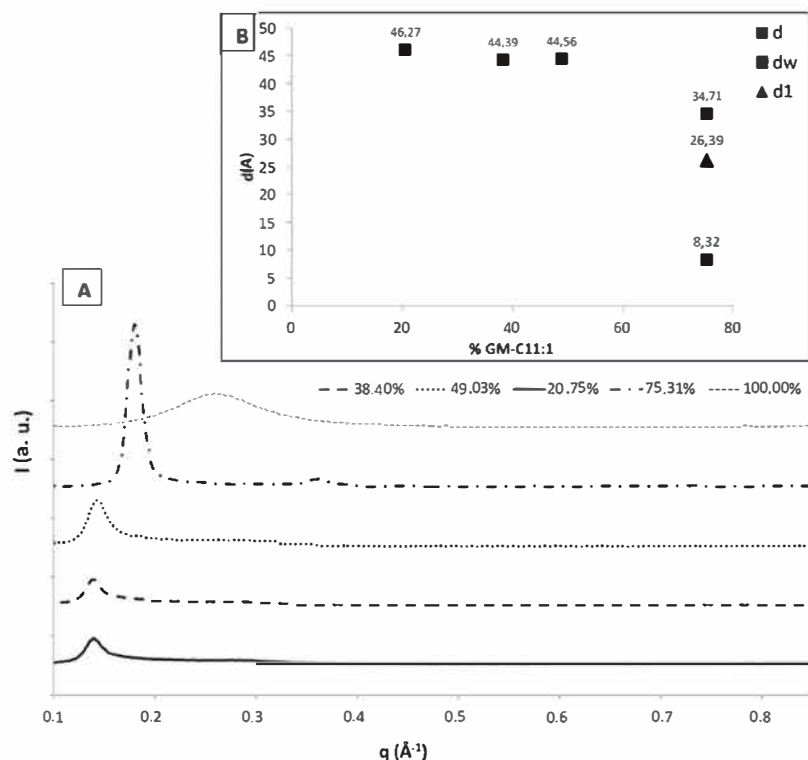


Figure 9. (A) X ray scattering profiles of GM C11:1/water system and (B) structural dimensions of the lamellar phase as a function of GM C11:1 concentration at 70 °C.

°C. Each sample was then subjected to two cycles of cooling from 50 to -80 °C at 5 °C/min and heating from -80 to 50 °C at 5 °C/min. Figure 7 shows the thermograms obtained for pure GM C11:1 and for a 60% (by mass) solution of GM C11:1 in ultrapure water. On cooling, the crystallization of GM C11:1 was characterized by two exothermic peaks, at 13.02 and -5.74 °C. On heating the melting of pure GM C11:1 was characterized by an endothermic peak at 45.6 °C corresponding to the melting of the most stable form. The 60% (by mass) solution of GM C11:1 displayed three crystallization peaks on cooling, at -16.01 , -16.19 , and -24.19 °C, and three endothermic peaks on heating, at 2.29, 19.87, and 23.12 °C. The cooling peak at -16.19 °C corresponds to the crystallization of the free water, and the heating peak at 2.29 °C corresponded to melting of the free water. The enthalpy value of the solid to liquid water transformation ($634.75 \text{ J} \cdot \text{g}^{-1} \cdot \text{K}^{-1}$) can be used to determine the content in free water, as explained later and reported in the Figure 8. The GM C11:1/water systems present polymorphous structures containing inserted water molecules, differing from the pure GM C11:1 system.

Figure 11 shows the variation in overall melting point of GM C11:1/H₂O systems as a function of their water content. This temperature corresponds to the Krafft temperature, the temperature at which these systems pass from a gelified state to a liquid crystal state.¹¹ Krafft temperature decreased from 47 to 22 °C for a decrease in GM C11:1 concentration from 91 to 60%. For concentrations below 50% (by mass), Krafft temperature stabilized at 25 °C.

The introduction of water decreases the physical stability of the gel system and has a plastifying effect.

The percentage of strongly bound water W (g of water per 100 g of water) was determined for each sample using the

method of Ambrosi et al.,⁵⁰ from the melting peak for pure water and the following equation

$$W = \left(\frac{333.79 - \Delta H_{\text{exp}}}{333.79} \right) \text{ and } N = \frac{M_n \times W}{M_w \times P} \times (100 - P)$$

where 333.79 J/g is the enthalpy of pure water,⁵³ ΔH_{exp} is the enthalpy measured experimentally for each sample, P is the concentration of GM C11:1, M_n and M_w are the molar masses of GM C11:1 and water, respectively, and N is the ratio between the number of moles of strongly bound water and GM C11:1.

Figure 8 shows the variation of W as a function of GM C11:1 content. Three zones are apparent: two extreme zones between 10 and 30% GM C11:1 and between 60 and 90% GM C11:1, in which the increase in water retention is linearly related to GM C11:1 content, and an intermediate zone. In the gels of the intermediate zone, the percentage of strongly bound water decreases linearly with increasing concentration. GM C11:1 is much better at retaining water than alkanoyl 6 O ascorbic acid esters,⁵⁰ for which a maximum of 24% of the water present is strongly bound at an ester concentration of 37%. The number of water molecules strongly bound per molecule of GM C11:1 decreases with increasing GM C11:1 concentration. GM C11:1 is, thus, less hydrated at higher concentrations. However, there may be an anomaly in the variation of W values because of a change in the degree of GM C11:1 hydration at these concentrations.

Small-Angle X-ray Scattering. The first phase diagrams of monoglyceride–water system were determined by Lutton,¹² from X ray diffraction measurements by Larsson.⁵⁴ The behavior of monoglycerides with water depends principally on the length of the alkyl chains and their saturated or unsaturated nature. All of the monoglycerides studied^{11,12} have

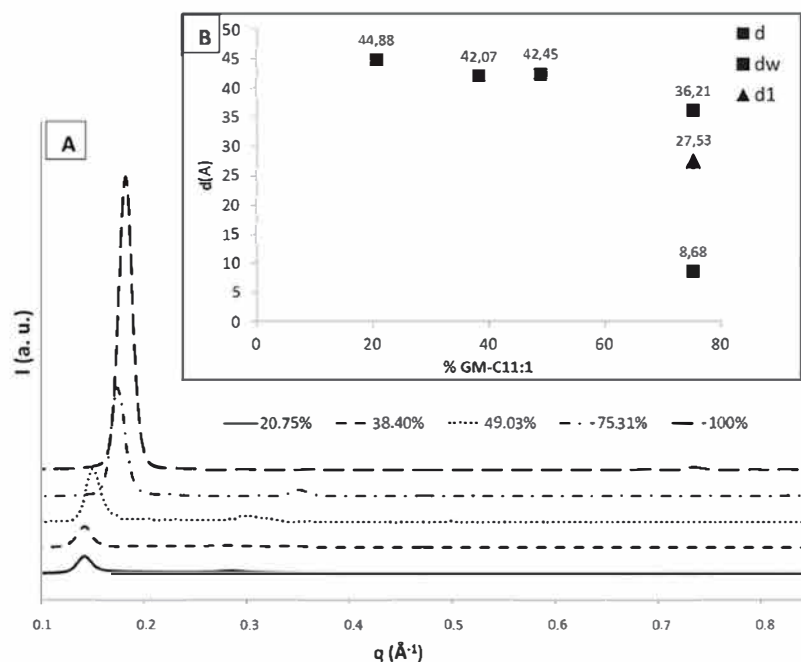


Figure 10. (A) X ray scattering profiles of GM C11:1/water system and (B) structural dimensions of the lamellar phase as a function of GM C11:1 concentration at 5 °C.

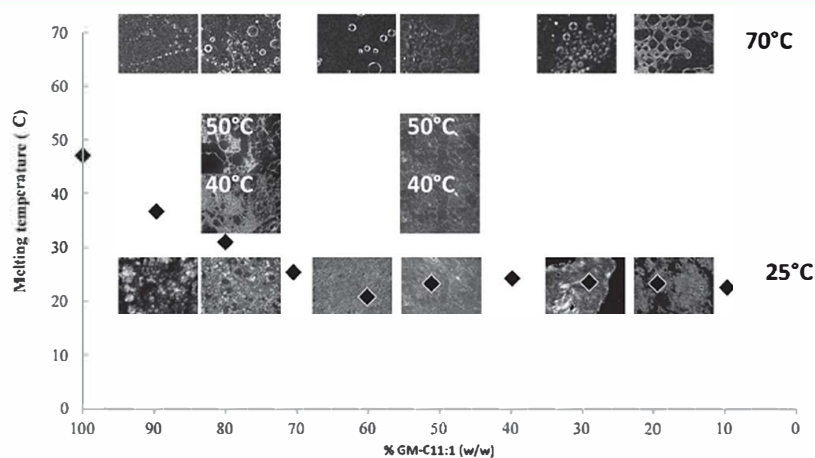


Figure 11. Influence of the percentage of GM C11:1 in water on melting temperature. Polarized light micrographs were obtained at 25 and 70 °C for all samples, and at 40 and 50 °C for 80 and 50% GM C11:1, respectively. ♦ indicates the Krafft temperature, except for 100% GM C11:1.

been found to have a lamellar zone in their phase diagrams: lamellar crystalline L_c phase, the lamellar gel L_β phase, and the lamellar liquid-crystalline L_α phase. At some concentrations, and at temperatures above the Krafft temperature, mono glycerides and water become organized into a lamellar L_α structure that swells with increasing water content. If the temperature increases sufficiently, this phase disappears and is replaced by cubic phases, liposomes, or an isotropic phase. If the lamellar system is cooled to below the Krafft temperature, a metastable gel L_β phase is obtained, as shown for GM C11:1 in Figure 9. The structure remains lamellar, even though the alkyl chains adopt a crystalline state. This gel L_β phase may last several days and gives rise to a coagel or a dehydrated crystal and water.⁴⁷

Lamellar Phase of the GM-C11:1/Water System. In the presence of water, GM C11:1 forms liquid crystals above the Krafft temperature, as shown in Figure 11. These liquid crystals

assemble into a lamellar L_α form, which can be rearranged into vesicles at 70 °C.

SAXS analysis of anhydrous crystalline GM C11:1 at 5 °C revealed the presence of lamellar symmetry, with a periodicity d (\AA) = $2\pi/q = 35.10 \text{ \AA}$ where q is the wave vector of the Bragg peak (Figure 10). The anhydrous sample analyzed had a melting temperature of 45 °C, corresponding to the β form (the most stable form), obtained by slow crystallization. As demonstrated by the polarized light micrographs, the gel, liquid crystal, and vesicular samples all had the lamellar structures L_β , L_α , and L_α respectively. The periodicity determined by SAXS for all GM C11:1 samples, thus, corresponds to the inter lamellar distance for each sample. The interlamellar distance of GM C11:1 ($d = 35.1 \text{ \AA}$) is very similar to that for glycerol 1 monoundecenoate reported by Malkin.⁵⁵ The lamellar organization of these two molecules is, therefore, very similar, despite their different melting points: 45 °C for GM C11:1 and 56.5 °C for the β form of glycerol 1 monoundecenoate.

SAXS analyses at 70 °C (Figure 9) indicated that, following the addition of water, the interlamellar distance increased for GM C11:1 concentrations of 49–75.3%, eventually stabilizing at higher water contents.

On cooling to 5 °C, which is below the Krafft temperature, the samples formed a metastable gel. The variation in interlamellar distance d with water content was similar to that for the same system analyzed in the liquid state at 70 °C. The tendency of these systems to swell has been reported before.^{12,52,56,57}

At 75% GM C11:1, the observed periodicity was very similar or even slightly higher in the gel phase than in the lamellar vesicle phase. The d_w and d_l distances were very similar in the gel and lamellar vesicle phases (Figures 9 and 10), indicating a similarity of the lamellar state in these two phases. The thickness of the GM C11:1 bilayer in the gel phase ($d_l = 26.4$ Å) is below the periodicity found in the anhydrous crystal ($d = 35.10$ Å). The lamellar assemblies of GM C11:1 in the lamellar vesicle and lamellar gel phases are, therefore, different from that in the anhydrous crystal phase. By contrast, the d_l values of the lamellar vesicle phase were expected to be close to the periodicity of GM C11:1 in the lamellar crystal phase, but this was not the case. If GM C11:1 behaves like saturated^{52,54,55} or monounsaturated⁵⁰ monoglycerides, then the periodicity of the anhydrous crystal should be lower, on the order of 26 Å, which is below that for glycerol decanoate ($d = 32.9$ Å⁵⁴), or the long distance periodicity d of the gel should be higher, at approximately 43.8 Å for 75% GM C11:1, as for glycerol monooleate.⁵²

This issue is of particular relevance, given that the molecular area of GM C11:1 in contact with water is 32.4 Å² in the gel phase and 33.7 Å² in the lamellar vesicle phase for the same concentration (75%) of GM C11:1. These values are similar to those obtained in the same concentration conditions for other lamellar gels and liquid crystals of monoglycerides, such as glycerol monooctanoate, glycerol monocaprylate, and glycerol monooleate, for which the molecular areas in contact with water are 30–35 Å².

Polarized light microscopy of samples at 25 and 70 °C demonstrated the presence of lamellar gels, regardless of water content. At 25 °C, the lamellar structures were in the gel state. At 70 °C, the lamellar structures were due to the formation of vesicles. At 40 and 50 °C, GM C11:1 displayed a liquid crystal lamellar structure, which was transformed into the vesicular system at 70 °C.

Based on the values for molecular area determined from SAXS data, we can calculate the number of water molecules present in the interlamellar space, using a value of 29.9 Å³ for the molecular volume of water. For the gel L_β phase, the volume of interlamellar water between two molecules of GM C11:1 is 268.9 Å³, corresponding to 4.5 molecules of water per molecule of GM C11:1. This value is greater than the number of strongly bound water molecules (3.8 molecules of water per molecule of GM C11:1) calculated from the DSC findings at the same concentration of GM C11:1. This indicates that the gels obtained are partially metastable: some of the water is free, and some (84.5%) is strongly bound. This value of 84.5% of water molecules strongly bound to the assembly, obtained by cross referencing SAXS and DSC data, is close to the results obtained solely on the basis of DSC (80.2% of water molecules strongly bound in the gel phase, at a GM C11:1 concentration of 75%).

For the vesicular phase, the volume of water was 279.7 Å³, corresponding to 4.7 molecules of water per molecule of GM C11:1. Here again, some of the molecules between layers are not strongly bound, with 81.0% of water molecules strongly bound, as estimated by cross referencing SAXS and DSC data.

■ CONCLUSIONS

A physicochemical study of GM C11:1 was carried out at different concentrations. We found that, in the dilute state, GM C11:1 assembled into aggregates in water, subsequently forming a monomolecular layer at both the liquid/air and liquid/solid interfaces, at concentrations above the CAC. Above this threshold concentration, GM C11:1 spontaneously formed vesicles in water. Such “dilute systems” could be used for emulsification and for the transport of lipophilic compounds in polar systems. Surface tension is low at the CAC, rendering GM C11:1 attractive as an interface active agent. The capacity of GM C11:1 to adsorb onto interfaces makes this molecule a potential candidate for the treatment of polar solid surfaces.

In a more concentrated state, GM C11:1 assembles into a lamellar form in water. By cross referencing SAXS and DSC findings, we were able to distinguish between the interlamellar water strongly bound to GM C11:1 and that remaining unbound and considered to be “mobile” water. The percentage of strongly bound water was proportional to the percentage of GM C11:1 in the system. In this case, GM C11:1 appears to be an effective molecule for surface treatments for which water retention is important.

The physicochemical characterization of GM C11:1, an amphiphilic molecule of vegetal origin, with the polar glycerol moiety and the lipophilic undecylenic chain, allows the classification of the molecule as a surface active agent of solvo surfactant type with a relatively high melting point, giving it the capacity to form hydrogels.

■ ASSOCIATED CONTENT

● Supporting Information

The Supporting Information is available free of charge on the ACS Publications website at DOI: [10.1021/acs.langmuir.6b03584](https://doi.org/10.1021/acs.langmuir.6b03584).

¹H NMR spectrum of GM C11:1 (PDF)

■ AUTHOR INFORMATION

Corresponding Author

*E mail: romain.valentin@ensiacet.fr. Phone: +33 534323524. Fax: +33 534323598.

ORCID

Romain Valentin: 0000 0002 5789 0740

Notes

The authors declare no competing financial interest.

■ ACKNOWLEDGMENTS

The authors would like to thank the French government and the Midi Pyrénées Region for their financial support through the Fond Unique Interministériel (FUI) and the CEPIA Department of INRA for support of the ANS program. The BIBS Microscopy facility of the Centre INRA at Nantes is acknowledged for providing access to the electron microscope, AFM, and Langmuir–Blodgett trough.

■ REFERENCES

- (1) Sheldon, R. A. Green and sustainable manufacture of chemicals from biomass: State of the art. *Green Chem.* 2014, 16, 950–963.
- (2) Meier, M. A. R.; Metzger, J. O.; Schubert, U. S. Plant oil renewable resources as green alternatives in polymer science. *Chem. Soc. Rev.* 2007, 36, 1788–1802.
- (3) Van der Steen, M.; Stevens, C. V. Undecylenic Acid: A Valuable and Physiologically Active Renewable Building Block from Castor Oil. *ChemSusChem* 2009, 2, 692–713.
- (4) Bigot, S.; Daghrir, M.; Mhanna, A.; Boni, G.; Pourchet, S.; Lecamp, L.; Plasseraud, L. Undecylenic acid: A tunable bio based synthon for materials applications. *Eur. Polym. J.* 2016, 74, 26–37.
- (5) Sagalowicz, L.; Leser, M. E.; Watzke, H. J.; Michel, M. Monoglyceride self assembly structures as delivery vehicles. *Trends Food Sci. Technol.* 2006, 17, 204–214.
- (6) Mouloungui, Z.; Rakotondrazafy, V.; Valentin, R.; Zebib, B. Synthesis of Glycerol 1 Monooleate by Condensation of Oleic Acid with Glycidol Catalyzed by Anion Exchange Resin in Aqueous Organic Polymorphic System. *Ind. Eng. Chem. Res.* 2009, 48, 6949–6956.
- (7) Grieser, F.; Drummond, C. J. The physicochemical properties of self assembled surfactant aggregates as determined by some molecular spectroscopic probe techniques. *J. Phys. Chem.* 1988, 92, 5580–5593.
- (8) Uchegbu, I. F.; Vyas, S. P. Non ionic surfactant based vesicles (niosomes) in drug delivery. *Int. J. Pharm.* 1998, 172, 33–70.
- (9) Kumar, G. P.; Rajeshwarao, P. Nonionic surfactant vesicular systems for effective drug delivery—An overview. *Acta Pharm. Sin. B* 2011, 1, 208–219.
- (10) Leser, M. E.; Sagalowicz, L.; Michel, M.; Watzke, H. J. Self assembly of polar food lipids. *Adv. Colloid Interface Sci.* 2006, 123–126, 125–136.
- (11) Krog, N.; Riisom, T.; Larsson, K. In *Encyclopedia of Emulsion Technology*; Becher, P., Ed.; Marcel Dekker, 1988; Vol. 2, p 321.
- (12) Lutton, E. S. Phase behavior of aqueous systems of monoglycerides. *J. Am. Oil Chem. Soc.* 1965, 42, 1068–1070.
- (13) Romain, V.; Ngakegni Limbili, A. C.; Mouloungui, Z.; Ouamba, J. M. Thermal Properties of Monoglycerides from *Nepheliumlappa ceum* L. Oil, as a Natural Source of Saturated and Monounsaturated Fatty Acids. *Ind. Eng. Chem. Res.* 2013, 52, 14089–14098.
- (14) Davies, J. T. A quantitative kinetic theory of emulsion type. I. Physical chemistry of the emulsifying agent. *Proceedings of the International Congress of Surface Activity*, 1957; Vol. 1, pp 426–438.
- (15) Marangoni, A. G.; Idziak, S. H. J.; Vega, C.; Batte, H.; Ollivon, M.; Jantzi, P. S.; Rush, J. W. E. Encapsulation structuring of edible oil attenuates acute elevation of blood lipids and insulin in humans. *Soft Matter* 2007, 3, 183–187.
- (16) Mouloungui, Z.; Gauvrit, C. Synthesis and influence of fatty acid esters on the foliar penetration of herbicides. *Ind. Crops Prod.* 1998, 8, 1–15.
- (17) Maruyama, T.; Niya, I.; Imamura, M.; Okada, M.; Matsumoto, T. Studies on Polymorphism of Monoglycerides. VI. Irregularities of Polymorphic Transition of Odd and Even Acid Monoglycerides. *Oil Chemistry* 1978, 27, 282–285.
- (18) Valentin, R.; Alignan, M.; Giacinti, G.; Renaud, F. N. R.; Raymond, B.; Mouloungui, Z. Pure short chain glycerol fatty acid esters and glyceric cyclocarbonic fatty acid esters as surface active and antimicrobial coagels protecting surfaces by promoting super hydrophilicity. *J. Colloid Interface Sci.* 2012, 365, 280–288.
- (19) Boussambe, G. N. M.; Valentin, R.; Mouloungui, Z. Structural Analysis of Partial and Total Esters of Glycerol Undecenoate and Diglycerol Undecenoate. *J. Am. Oil Chem. Soc.* 2015, 92, 1567–1577.
- (20) Luzzati, V. In *Biological Membranes*; Chapman, D., Ed.; Academic Press: New York, 1968; pp 71–123.
- (21) Fontell, K.; Mandell, L.; Mehtinen, H.; Ekwall, P. Three component system sodium caprylate–decanol–water: II. Densities of the various phases and the partial specific volumes of the components. *Acta Chem. Scand.* 1968, 74, 1–20.
- (22) Queste, S.; Bauduin, P.; Touraud, D.; Kunz, W.; Aubry, J. M. Short chain glycerol 1 monoethers—A new class of green solvo surfactants. *Green Chem.* 2006, 8, 822–830.
- (23) Lunkenheimer, K.; Schrödle, S.; Kunz, W. Dowanol DPnB in water as an example of a solvo surfactant system: Adsorption and foam properties. In *Trends in Colloid and Interface Science XVII*; Springer: Berlin, Heidelberg, 2014; pp 14–20.
- (24) Sánchez, C. C.; Niño, M. R. R.; Patino, J. M. R. Relaxation phenomena in monoglyceride films at the air–water interface. *Colloids Surf., B* 1999, 12, 175–192.
- (25) Rangelov, S.; Momekova, D.; Almgren, M. Structural characterization of lipid based colloidal dispersions using cryogenic transmission electron microscopy. In *Microscopy: Science, Technology, Applications and Education*; Mendez Vilas, A., Diaz, J., Eds.; Formatex Research Center, 2010; pp 1724–1734.
- (26) Danino, D. Cryo TEM of soft molecular assemblies. *Curr. Opin. Colloid Interface Sci.* 2012, 17, 316–329.
- (27) Klaus, A.; Tiddy, G. J. T.; Touraud, D.; Schramm, A.; Stühler, G.; Drechsler, M.; Kunz, W. Phase Behavior of an Extended Surfactant in Water and a Detailed Characterization of the Dilute and Semidilute Phases. *Langmuir* 2010, 26, 5435–5443.
- (28) Momekova, D.; Momekov, G.; Rangelov, S.; Storm, G.; Lambov, N. Physicochemical and biopharmaceutical characterization of dipalmitoyl phosphatidylcholine liposomes sterically stabilized by copolymers bearing short blocks of lipid mimetic units. *Soft Matter* 2010, 6, 591–601.
- (29) Uchegbu, I. F.; Florence, A. T. Non ionic surfactant vesicles (niosomes): Physical and pharmaceutical chemistry. *Adv. Colloid Interface Sci.* 1995, 58, 1–55.
- (30) El Kirat, K.; Burton, L.; Dupres, V.; Dufrene, Y. F. Sample preparation procedures for biological atomic force microscopy. *J. Microsc.* 2005, 218, 199–207.
- (31) Patino, J. M. R.; Sánchez, C. C.; Niño, M. R. R. Morphological and Structural Characteristics of Monoglyceride Monolayers at the Air–Water Interface Observed by Brewster Angle Microscopy. *Langmuir* 1999, 15, 2484–2492.
- (32) Patino, J. M. R.; Sánchez, C. C.; Niño, M. R. R.; Fernández, M. C. Structural Dilatational Characteristics Relationships of Monoglyceride Monolayers at the Air–Water Interface. *Langmuir* 2001, 17, 4003–4013.
- (33) Pezron, I.; Pezron, E.; Claesson, P. M.; Bergenstahl, B. A. Monoglyceride surface films: Stability and interlayer interactions. *J. Colloid Interface Sci.* 1991, 144, 449–457.
- (34) Park, Y.; Choi, Y. W.; Park, S.; Cho, C. S.; Fasolka, M. J.; Sohn, D. Monolayer formation of PBLG–PEO block copolymers at the air–water interface. *J. Colloid Interface Sci.* 2005, 283, 322–328.
- (35) Paria, S.; Khilar, K. C. A review on experimental studies of surfactant adsorption at the hydrophilic solid–water interface. *Adv. Colloid Interface Sci.* 2004, 110, 75–95.
- (36) Brinck, J.; Jönsson, B.; Tiberg, F. Kinetics of Nonionic Surfactant Adsorption and Desorption at the Silica–Water Interface: One Component. *Langmuir* 1998, 14, 1058–1071.
- (37) Brinck, J.; Jönsson, B.; Tiberg, F. Kinetics of Nonionic Surfactant Adsorption and Desorption at the Silica–Water Interface: Binary Systems. *Langmuir* 1998, 14, 5863–5876.
- (38) Tiberg, F. Physical characterization of non ionic surfactant layers adsorbed at hydrophilic and hydrophobic solid surfaces by time resolved ellipsometry. *J. Chem. Soc., Faraday Trans.* 1996, 92, 531–538.
- (39) Tiberg, F.; Joesson, B.; Lindman, B. Ellipsometry Studies of the Self Assembly of Nonionic Surfactants at the Silica–Water Interface: Kinetic Aspects. *Langmuir* 1994, 10, 3714–3722.
- (40) Pagac, E. S.; Prieve, D. C.; Tilton, R. D. Kinetics and Mechanism of Cationic Surfactant Adsorption and Coadsorption with Cationic Polyelectrolytes at the Silica–Water Interface. *Langmuir* 1998, 14, 2333–2342.
- (41) Partyka, S.; Zaini, S.; Lindheimer, M.; Brun, B. The adsorption of non ionic surfactants on a silica gel. *Colloids Surf.* 1984, 12, 255–270.
- (42) Nevskaiia, D. M.; Guerrero Ruiz, A.; López González, J. d. D. Adsorption of Polyoxyethylene Surfactants on Quartz, Kaolin, and

Dolomite: A Correlation between Surfactant Structure and Solid Surface Nature. *J. Colloid Interface Sci.* 1996, 181, 571–580.

(43) Levitz, P.; Van Damme, H. Fluorescence decay study of the adsorption of nonionic surfactants at the solid liquid interface. 2. Influence of polar chain length. *J. Phys. Chem.* 1986, 90, 1302–1310.

(44) Sato, K. Crystallization behaviour of fats and lipids—A review. *Chem. Eng. Sci.* 2001, 56, 2255–2265.

(45) Allais, C.; Keller, G.; Lesieur, P.; Ollivon, M.; Artzner, F. X ray diffraction/Calorimetry coupling. *J. Therm. Anal. Calorim.* 2003, 74, 723–728.

(46) Metin, S.; Hartel, R. *Crystallization of Fats and Oils*; Shahidi, F., Eds.; John Wiley & Sons Inc., 2005.

(47) Sein, A.; Verheij, J. A.; Agterof, W. G. M. Rheological characterization, crystallization, and gelation behavior of monoglyceride gels. *J. Colloid Interface Sci.* 2002, 249, 412–422.

(48) Fong, C.; Wells, D.; Krodkiewska, I.; Booth, J.; Hartley, P. G. Synthesis and mesophases of glycerate surfactants. *J. Phys. Chem. B* 2007, 111, 1384–1392.

(49) Chupin, V.; Boots, J. W. P.; Killian, J. A.; Demel, R. A.; de Kruijff, B. Lipid organization and dynamics of the monostearoylglycerol–water system. A 2H NMR study. *Chem. Phys. Lipids* 2001, 109, 15–28.

(50) Ambrosi, M.; Nostro, P. L.; Fratoni, L.; Dei, L.; Ninham, B. W.; Palma, S.; Manzo, R. H.; Allemandi, D.; Baglioni, P. Water of hydration in coagels. *Phys. Chem. Chem. Phys.* 2004, 6, 1401–1407.

(51) Shibukawa, M.; Aoyagi, K.; Sakamoto, R.; Oguma, K. Liquid chromatography and differential scanning calorimetry studies on the states of water in hydrophilic polymer gel packings in relation to retention selectivity. *J. Chromatogr. A* 1999, 832, 17–27.

(52) Pezron, I.; Pezron, E.; Bergenstaahl, B. A.; Claesson, P. M. Repulsive pressure between monoglyceride bilayers in the lamellar and gel states. *J. Phys. Chem.* 1990, 94, 8255–8261.

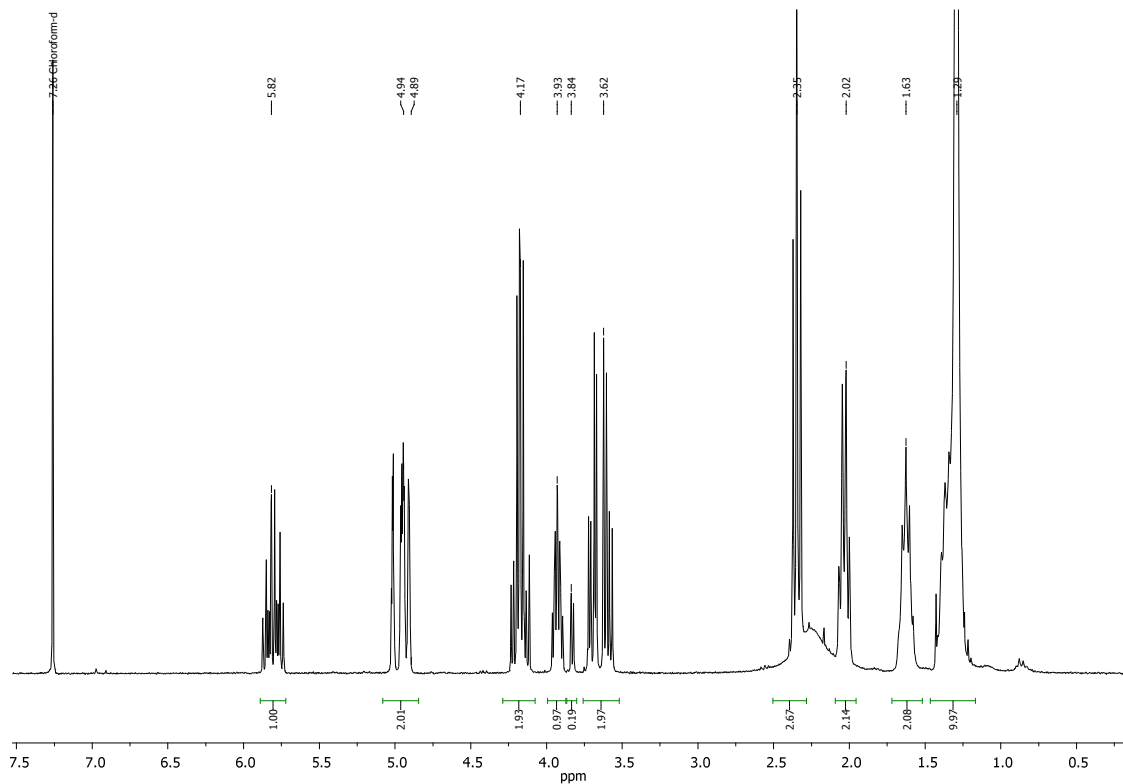
(53) Dean, J. A. *Lange's Handbook of Chemistry*, 5th ed.; Mc Graw Hill, Inc., 1999.

(54) Larsson, K. The Structure of Mesomorphic Phases and Micelles in Aqueous Glyceride Systems. *Z. Phys. Chem.* 1967, 56, 173–198.

(55) Malkin, T.; Shurbagy, M. R. E. An X ray and thermal examination of the glycerides. Part II. The α monoglycerides. *J. Chem. Soc.* 1936, 1628–1634.

(56) Lutton, E. S. The phases of saturated 1 monoglycerides C14–C22. *J. Am. Oil Chem. Soc.* 1971, 48, 778–781.

(57) Malkin, T. The polymorphism of glycerides. *Prog. Chem. Fats Other Lipids* 1954, 2, 1–50.



Proton NMR spectrum of GM-C11:1 recorded on a Fourier 300 (300 MHz) spectrometer (Bruker, Karlsruhe, Germany). The acquisition temperature was set to 300 K. The sample was dissolved in deuterated chloroform (CDCl₃). Chemical shifts were determined with tetramethylsilane at 0 ppm (TMS) as the reference.